Focussed on Multiaxial Fatigue and Fracture

Prediction of the critical stress to crack initiation associated to the investigation of fatigue small crack

D. Marhabi
H.E.I 13 Rue de TOUL 59046 Lille-cedex France
driss.marhabi@hei.fr

N. Benseddiq, G. Mesmacque
University Lille 1 Villeneuve d'Ascq France
noureddine.benseddiq@univ-lille1.fr
gerard.mesmacque@univ-lille1.fr

Z. Azari
LaBPS, ENIM, 1 Route d'Ars Laquenexy, 57070 Metz, France
azari@enim.fr

J.M. Nianga
H.E.I 13 Rue de TOUL 59046 Lille-cedex France
Jean-Marie.NIANGA@hei.fr

ABSTRACT. Fatigue design is of vital importance to avoid fatigue small crack growth in engineering structures. This study shows that the critical fatigue design stress can be defined below the usual endurance limit, considered in rules and codes. The material constitutive behaviour is using linear isotropic elasticity.

Lassere and Pallin-Luc [1-2] use the elastic energy and over-energy under uniaxial load (tension and rotating bending). The authors deduce the influencing critical stress value corresponding to σ*. It's a linear approach.

We propose an over-energy under dissymmetrical rotating bending and expressed in the ellipse axes. An asymptotic approach is transformed the over-energy in polynomial function of critical stress. Unknown depend on experimental service conditions, endurance limit of tension and rotating bending of specimen. The fatigue database of 30NCD16 steel studied by Froustey and Dubar [3-13] is used. Critical stresses are evaluated (Fig. 2).

The research done by Manning and all [4] has shown the small crack effect to be as large as 0.3 mm. Small crack and critical stress are illustrated here in as resulting from pure bending approach expressed by Bazant law [7]. It's reproduces well the Kitagawa diagram [6] (Fig. 3).

When the short cracks are hidden in the material, we shows that the number

cycles during small crack growth be significantly higher (Fig. 4) than the corresponding cycles of large cracks growth (ONI's fatigue test) for the same physically crack size. Indeed its evolution can be blocked by a microstructural barrier (grain boundary, for example). Hence, the considerations of small crack growth are strongly influencing the fatigue life of a component or structure.

KEYWORDS. Tensile; Dissymmetrical rotating bending; Over-energy; Critical stress; Small crack; Fatigue cycle.

INTRODUCTION

D ue to fatigue loading cracks can initiate in material. They can exist as a consequence of manufacturing process such as (deep machining marks, voids in welds) or of metallurgical and geometrical discontinuities. Small cracks have been thoroughly studied aerospace, nuclear, and the ground vehicle industries. In order to predict defects and/or transverse cracks under service conditions, different cracking process have to be noted and explained in terms of the fatigue small crack effect.

The first part of this paper is dedicated to analyze the over-energy under dissymmetrical rotating bending and expressed in the ellipse support. An Asymptotic approach associated to critical stress function predict and evaluate the unknown stresses σ*. The second part proposes the small crack size effect using pure bending approach and Bazant law. We confirm that the curve trend reproduces well the Kitagawa diagram. The last part is considering the applicability of linear elastic fracture mechanics (LEFM) for physically small crack. The Integral calculus of number cycles required for small crack is determined. However, the small crack has faster growth rates than long crack.

THE INFLUENCING STRESS IN THE FATIGUE IN THE FATIGUE INITIATION CRACK

A s proposed by Palin-Luc, Lasserre and Banvillet [1-2] to predict the effect on the fatigue under a uniaxial load in the component. An area influencing fatigue crack initiation S* is considered. From fully reversed fatigue, these authors show that a stress σ* can be defined below the endurance limit σ_{-1}. The critical stress limit σ* is associated to no damage crack.

The Elastic Energy and Over-Energy

In this study we assume that the material's behaviour law is linear isotropic elasticity. For a given elementary area of material, the energy density per loading cycle is:

$$\mathrm{W} = \frac{1}{T} \int_T \left\langle \frac{1}{2} \sigma_{ij}(M,t) \cdot \varepsilon_{ij}(M,t) \right\rangle dt \tag{1a}$$

The energy W_{Te} and W_{Rb} distributions are axisymmetric in tensile and rotating bending. These sinusoidal loadings are taking as a reference to identify the critical stress σ^*.

S* is the area influencing fatigue crack initiation.

$$S*(C) = \left\{ P(x,y) \quad around \quad C \quad so \quad that \quad W(P) \geq W^*(C) \right\} \tag{1b}$$

The over-energy $\omega(C)$ allows initiating short cracks around the critical point C

$$\omega(C) = \frac{1}{S^*(C)} \iint_{S^*(C)} (W(M) - W^*(C)) ds \tag{1c}$$

At the endurance limit, this quantity $\omega(C)$ is supposed to be constant. If we note ω_{Uniax}^{D} as being its value at the endurance limit for any uniaxial stress our criterion is:

$$\omega(C) < \omega_{Uniax}^{D} \tag{1d}$$

Postulate: The quantity ω is an intrinsic size in the material (noted ω_{Uniax}) thus it does not depend on the loading type. We can identify their energy to satisfy the equation:

$$W_{Uniax} = W_{Te} = W_{Rb} = W_{Pb} == W_{Rb,d} \tag{2a}$$

$$\omega_{Uniax}^{D} = \omega_{Te} = \omega_{Rb} = \omega_{Pb} = \omega_{Rb,d} \tag{2b}$$

Uniaxial Energy Associated to critical stress

By reference to an homogenous fully reversed uniaxial stress and the energy analyses by Palin-Luc, Lasserre and Banvillet (Eqs. 1a and 1c). The authors deduce the influencing critical stress value corresponding to σ* in the fatigue initiation crack:

$$\sigma_{Eq}^{*} = \sqrt{2\sigma_{Eq,Te}^{2} - \sigma_{Eq,Rb}^{2}} \tag{3}$$

From (Eqs. 1a and 1c) and value at the endurance limit for (Eq. 3) it easy to prove that W_{Uniax}^{*} is given by (4b); ω_{Uniax}^{D} can be calculated by (4c).

$$\begin{cases} \sigma_{Eq}^{*} = \sqrt{2(\sigma_{Te,-1})^{2} - (\sigma_{Rb,-1})^{2}} & (4a) \\[2mm] W_{Uniax}^{*} = \dfrac{2(\sigma_{Te,-1})^{2} - (\sigma_{Rb,-1})^{2}}{4E} & (4b) \\[2mm] \omega_{Uniax}^{D} = \dfrac{(\sigma_{Rb,-1})^{2} - (\sigma_{Te,-1})^{2}}{4E} & (4c) \end{cases}$$

ENERGY UNDER DISSYMMETRICAL ROTATING BENDING

The service stress (Fig. 1 (5a) (b)) on a straight section by a cylindrical specimen:

$$\sigma_{Rb,d}(t) = \sigma_{m,Rb}\frac{y}{R} + \sigma_{Rb}\frac{r}{R} \cdot \sin \omega t \tag{5a}$$

The energy density given to each elementary under dissymmetrical rotating bending is:

$$W_{Rb,d} = \frac{\sigma_{m,Rb}^{2}}{4E}\left(\frac{y}{R}\right)^{2} + \frac{\sigma_{Rb}^{2}}{4E}\left(\frac{r}{R}\right)^{2} \tag{5b}$$

The energy value corresponding to σ* for fatigue initiation crack is represented by:

$$W^*_{Rb,d} = \frac{\sigma^2_{m,Rb}}{4E}\left(\frac{y^*}{R}\right)^2 + \frac{\sigma^2_{Rb}}{4E}\left(\frac{r^*}{R}\right)^2 = W^*_{Uniax} = \frac{2(\sigma_{Te,-1})^2 - (\sigma_{Rb,-1})^2}{4E} \tag{5c}$$

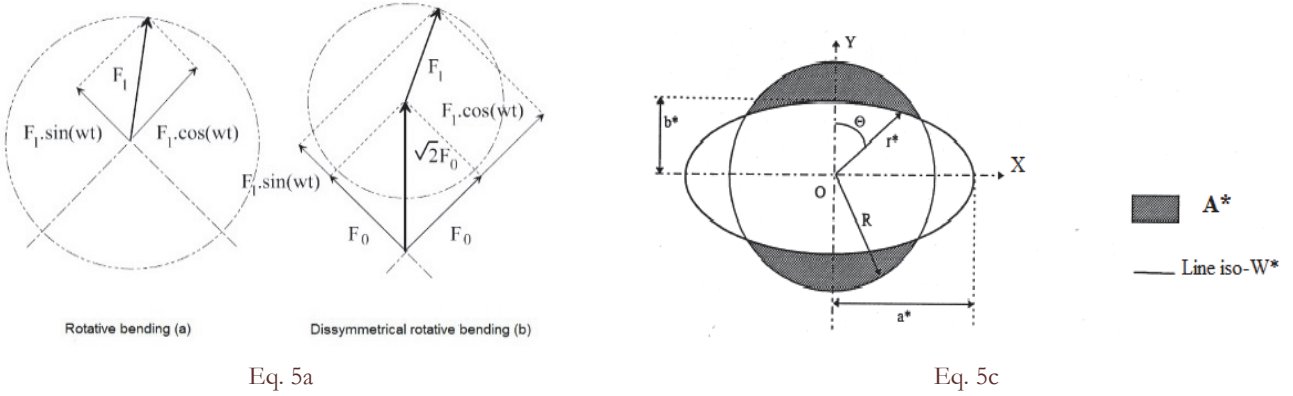The Iso-energy (Eq. 5c) is an ellipse on the cross-section of the specimen (Fig. 1).

Eq. 5a   Eq. 5c

Figure 1: Dissymmetrical rotating bending (Eq. 5a) and line Iso-energy W^* (Eq. 5c).

The large half axis a^* and the small half axis b^* defined by (Eq. 5c) are the ellipse axes:

$$\left(\frac{b^*}{R}\right)^2 = \frac{2\sigma_{Te,-1}^2 - \sigma_{Rb,-1}^2}{\sigma^2_{Rb,m} + \sigma^2_{Rb}} \tag{6a}$$

$$\left(\frac{a^*}{R}\right)^2 = \frac{2(\sigma_{Te,-1})^2 - (\sigma_{Rb,-1})^2}{\sigma^2_{Rb}} \tag{6b}$$

Over-Energy under Dissymmetrical Rotating Bending (D.R.B) in the Ellipse Axes
This part is dedicated to analyze the over-energy expressed in the ellipse support is:

$$\omega_{RB,d} = \frac{\int_{S^*} W_{Rb,d}\, ds}{S^*} - W^*_{Uniax} = \frac{I_{ce}}{\pi R^2\left[1 - \left(\frac{b^*}{R}\right)\left(\frac{a^*}{R}\right)\right]} - \frac{2\sigma_{Te,-1}^2 - \sigma_{Rb,-1}^2}{4E} \tag{7a}$$

The member term I_{ce} is given by:

$$I_{ce} = \iint_{S_c} W_{Rb,d}(y,r)\, dy\, dr - \iint_{S_e} W_{Rb,d}(y,r)\, dy\, dr = I_c - I_e \tag{7b}$$

S_c and S_e are respectively the circular and the elliptical section (Fig. 1 (5c))
The Integral transformation in elliptical section gives

$$I_e = \int_{0}^{1} \int_{-\pi}^{+\pi} \frac{1}{4} \left\{ \frac{\sigma_{m,Rb}^2}{E} \left(\frac{b^*}{R} \right)^2 \cos^2 \theta + \frac{\sigma_{Rb}^2}{E} \left(\left(\frac{b^*}{R} \right)^2 \cos^2 \theta + \left(\frac{a^*}{R} \right)^2 \sin^2 \theta \right) \right\} \left(\frac{a^*}{R} \right) \left(\frac{b^*}{R} \right) u^3 du d\theta =$$

$$= \frac{\pi R^2}{8} \left(\left(\frac{a^*}{R} \right)^3 \left(\frac{b^*}{R} \right) \frac{\sigma_{Rb}^2}{E} + \left(\frac{a^*}{R} \right) \left(\frac{b^*}{R} \right)^3 \right) \frac{\sigma_{Eq,Rb}^2}{E} \right)$$

(7c)

The Integral transformation in circular section evaluated by

$$I_c = \int_{0}^{1} \int_{-\frac{\pi}{2}}^{+\frac{\pi}{2}} \frac{1}{4} \left[\frac{\sigma_{m,Rb}^2}{E} \frac{1}{2} (1 - \cos 2\theta) + \frac{\sigma_{Rb}^2}{E} (1 + \sin 2\theta) \right] u^3 du d\theta = \frac{\pi R^2}{8} \left[\frac{\sigma_{m,Rb}^2}{E} + \frac{2\sigma_{Rb}^2}{E} \right]$$

(7d)

The over-energy (7a) under dissymmetrical rotating bending when $\dfrac{a^*}{R} < 1$, gives:

$$\omega_{Rb,d} = \frac{\left\{ (\sigma_{m,Rb}^2 + 2\sigma_{Rb}^2) - \left\{ \sigma_{Rb}^2 \left(\frac{a^*}{R} \right)^3 \left(\frac{b^*}{R} \right) + \sigma_{Eq,Rb}^2 \left(\frac{a^*}{R} \right) \left(\frac{b^*}{R} \right)^3 \right\} \right\}}{8E \left[1 - \left(\frac{b^*}{R} \right) \left(\frac{a^*}{R} \right) \right]} - \frac{2\sigma_{Te,-1}^2 - \sigma_{Rb,-1}^2}{4E}$$

(8)

For us, this result is necessary to identify critical crack in the cylindrical specimen.

An Asymptotic Method and over-Energy expressed by Critical Stress

The basic concept in the influence area of no damage crack is expressed by $w_{Te}^* = w_{Rb,d}^*$ We allow writing two limits equations near the small half axis and the large half axis of the ellipse (Fig. 1). With this asymptotic method, we have:

$$\begin{cases} For \qquad \theta = 0, \ \ \sigma_{Eq}^{*\,2} = (\sigma_{Eq,Rb}^2) \left(\frac{b^*}{R} \right)^2 \\[4mm] For \qquad \theta = \frac{\pi}{2}, \ \ \sigma_{Eq}^{*\,2} = (\sigma_{Rb}^2) \left(\frac{a^*}{R} \right)^2 \end{cases}$$

(9)

The equality (8) and (9) are considered to define the critical stress Eq. (10). It can be deduced by the application of the postulate (Eq. 2b):

$$\omega_{Rb,d} - \omega_{Te} = A_{Rb} \left(\sigma_{Eq}^{*\,2} \right)^2 + B_{Rb} \left(\sigma_{Eq}^{*\,2} \right) + C_{Rb} = 0$$

(10a)

$$A_{Rb} = 6$$

$$B_{Rb} = -4 * [(2\sigma_{Te,-1}{}^{2} - \sigma_{Rb,-1}{}^{2}) + (\sigma_{Eq,Rb})\sigma_{Rb} + (\sigma_{Eq,Te}^{2})] \quad (10b)$$

$$C_{Rb} = [4 * [(\sigma_{Eq,Te}^{2}) + (2\sigma_{Te,-1}{}^{2} - \sigma_{Rb,-1}{}^{2}) - \sigma_{Eq,Rb}^{2} - \sigma_{Rb}{}^{2}](\sigma_{Eq,Rb}\sigma_{Rb})$$

From the Eq. (10a) according to the postulate energy and (Eq. 9) we define:

$$\begin{cases} Database \begin{cases} \sigma_{m,Rb} \\ \sigma_{Rb} \end{cases} \\ \\ \sigma_{Te} = 427\, MPa \\ \sigma_{m,Te} = 290\, MPa \\ \sigma_{Rb,-1} = 658\, MPa \\ \sigma_{Te,-1} = 560\, MPa \end{cases} \Rightarrow \begin{cases} \sigma_{Eq}^{*}{}^{2} = \dfrac{-B_{Rb} \pm \sqrt{B_{Rb}{}^{2} - 4A_{Rb}C_{Rb}}}{2A_{RB}} \end{cases} \quad (11)$$

Prediction of the Critical Stress
Our proposal consists to study an analytical model and predict the critical stress:

$$\omega(\sigma_{Eq}^{*}) = A_{Rb}\left(\sigma_{Eq}^{*}{}^{2}\right)^{2} + B_{Rb}\left(\sigma_{Eq}^{*}{}^{2}\right) + C_{Rb} \quad (12)$$

We use the fatigue database of 30NCD16 steel [3-13]. The endurance limit $\sigma_{Te,-1}^{D}, \sigma_{Fr,-1}^{D}$ and various stresses values σ_{Rb} and $\sigma_{m,Rb}$ identify the roots by (Eq.12).
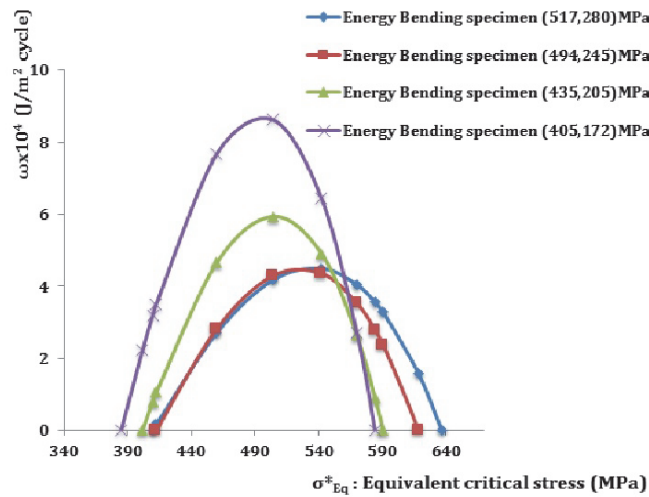

Figure 2: Over-energy (D.R.B) for various stress values of 30NCD16 steel.

The critical stresses of any curve in Tab. 1 are situated between σ* and σ₋₁ and designed respectively by the stress of small crack σ*min and the stress of the smallest crack σ*max.
The over-energy allows for the critical stress and requires a vigilance on the fatigue design in engineering structures.

	Specimen 1		Specimen 2		Specimen 3		Specimen 4	
	σ_{Rb}	σ_m	σ_{Rb}	σ_m	σ_{Rb}	σ_m	σ_{Rb}	σ_m
Bending stress (MPa)	517	280	494	245	435	205	405	172
Critical stress σ^*_{min}	289.57		293.29		278.02		253.03	
Critical stress σ^*_{max}	566.83		545.97		514.46		508.80	

Table 1: Critical stress in a smooth cylindrical specimen.

FATIGUE SMALL CRACK ASSOCIATED TO CRITICAL STRESS

In 1976, Kitagawa [6] presented a schematic comparison between stress range and crack length a, on a log-log scale. In this part, we approximate the small crack size for various stress σ* under pure bending and expressed by Bazant's law [7].

Small Crack effect and Critical Stress under a Pure Bending
The elasticity theory [5] evaluate the crack size under influencing stress σ*:

$$a = \left(\frac{\Delta K_{th}}{1.99 \times \sigma^*} \right)^2 \tag{13a}$$

The fatigue limit ratios is based on the Mises criterion $\frac{\sigma^*}{\sigma^n} \sim \frac{3}{5}$. Indeed, the crack length a under a pure bending (Fig. (5a)) is:

$$a = \left(\frac{5}{3} \frac{\Delta K_{th}}{1.99 \times \sigma_{Rb}} \right)^2 \tag{13b}$$

We hold the service conditions values from database of Froustey and Dubar.

Bazant's Law for Small Crack
If critical stress cannot lead to long crack growth prediction, the method used is Bazant's law for cracked material. Since the process is controlled by critical stress σ*, the fatigue limit ratios is $\frac{5}{3}$ and the normal stress effect law proposed is:

$$\sigma^n(a) = \frac{5}{3} * \left(\frac{\Delta K_{th}}{\sqrt{\pi a}} \right) \left(1 + \left(\frac{a_{th}}{a} \right)^{\frac{\gamma}{2}} \right)^{-\frac{1}{\gamma}} \tag{13c}$$

According to Tanaka [8] and Livieri [9], most of experimental data is situated between two corresponding curves in γ = 1.25 and γ = 8. The threshold stress in the literature for 30NCD16 steel have average values between 4.3 MPa√m and 6 MPa√m. In our analyses we used $\Delta K_{th} = 6$ MPa√m and $a_{th} = 0.1 mm$. The representation of (Eqs. 13b and 13c) gives:
The small crack effect is illustrated here in as resulting from Bazant's law and reproduces well the Kitagawa diagram. We show also that the curve predicted by (Eq. 13b) is significantly bounded by the Bazant curves (Eq. 13c). The small crack a_0 length below which the linear elastic fracture mechanics (LEFM) considered is the first point where the Bazant curve (γ = 8) detaches from the endurance line. The initiation crack length predicted (Fig. 3) is $a_0 = 40.E-6$ m
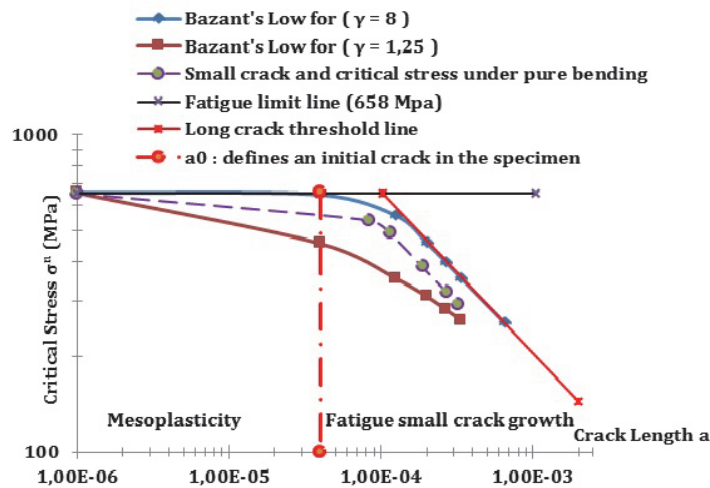
Figure 3: Small crack effect for 30NCD16 steel under critical stress.

PREDICTION OF THE FATIGUE CYCLES AND LEFM ANALYSES

The initiation behavior of small crack is more complex than long crack propagation. Based on the general classification of small fatigue cracks as defined in ASTM standard E647 [10], small cracks are defined as follows:
- **Microstructurally small** if their length is comparable to the microstructural scale,
- **Mechanically small** if their length is small compared to the scale of local plasticity,
- **Physically small** if their length is typically between 0.1 and a_ℓ = 2mm [4-10].
We consider the applicability of (LEFM) for physically small crack when $a_0 \le a \le a_\ell$.

Paris-Erdogan Law and Parameters (C, m) in Kinetics Region I
The pure bending approach (Eq. 13b) suggests the existence of small crack under critical stress in high strength steel 30NCD16 used in the aerospace industry. It is therefore important to predict the number cycles of such defects in Kinetics region I under shear stress σ^*. The Paris-Erdogan law is:

$$\frac{da}{dN} = C \cdot (\Delta K)^m \qquad \text{(da/dN in m/cycles et } \Delta K \text{ in MPa}\sqrt{m}\text{)} \tag{14a}$$

Where $\Delta K = \Delta K_{th}(1+(\frac{a_{th}}{a})^{\frac{\gamma}{2}})^{-\frac{1}{\gamma}} \alpha$ and α is a function of a [6] $\alpha(a) = \frac{3}{5}\frac{K_{max}}{\sigma^* \sqrt{\pi a}}$

The relationship (Eq. 14a) between the rate small crack and the stress intensity factor is:

$$\frac{da}{dN} = C \cdot \left(\frac{K_{max}}{\frac{5}{3}\sigma^* \sqrt{\pi a}} \Delta K_{th}(1+(\frac{a_{th}}{a})^{\frac{\gamma}{2}})^{-\frac{1}{\gamma}} \right)^m \tag{14b}$$

For this situation, the integration is usually necessary using either computer programs.
The fatigue HENAFF's [11] test result for 30NCD16 steel in the first part of Kinetics region I enable us to calculate the parameters C and m:

$\left[\Delta K, \dfrac{da}{dN}\right]$	$[C, m]$
1^t point: $(2.8, 8\ 10^{-11})$ 2^d point: $(3, 1.25\ 10^{-10})$	$[1.028\ 10^{-13}, 6.468]$
1^t point: $(3, 3\ 10^{-10})$ 2^d point: $(3.25, 4\ 10^{-10})$	$[5.718\ 10^{-12}, 3.594]$
1^t point: $(3.5, 6\ 10^{-10})$ 2^d point: $(3.9, 10^{-9})$	$[1.626\ 10^{-12}, 4.716]$

Table 2: The parameters C and m in Kinetics region I.

Prediction of Numbers Cycles for Physically Small Crack

The relationship (Eq. 14b) is integrated in interval $[a_0, a_p]$ when $a_p \le a_\ell$ (p=1, 2, ... , n). The number cycles of small crack growth is:

$$N_f = \frac{1}{C}\left(\frac{5}{3}\frac{\sigma^*}{K_{max}\ \Delta K_{th}}\right)^m \int_{a_0}^{a_p} \sqrt{(\pi a)^m}\left(1+\left(\frac{a_{th}}{a}\right)^{\frac{\gamma}{2}}\right)^{\frac{m}{\gamma}} da \qquad (15)$$

a_0: defines the intergranular initial crack length in the specimen.

a_ℓ: defines the upper limit of physically small cracks.

The analysis for the fatigue life use the parameter $\gamma = 6$. The crack grows under the fracture toughness of the material $K_{max} = 18$ MPa√m. The thresholds stress intensity used in this analyze is: $\Delta K_{th} = 6$ MPa√m and $a_{th} = 0.1mm$. The parameters C and m of Tab. 2 in Kinetics region I are used. The mean defect (inclusion whose size is $a_0 = 40 \times 10^{-6}$ m) was assumed to exist in the specimen.

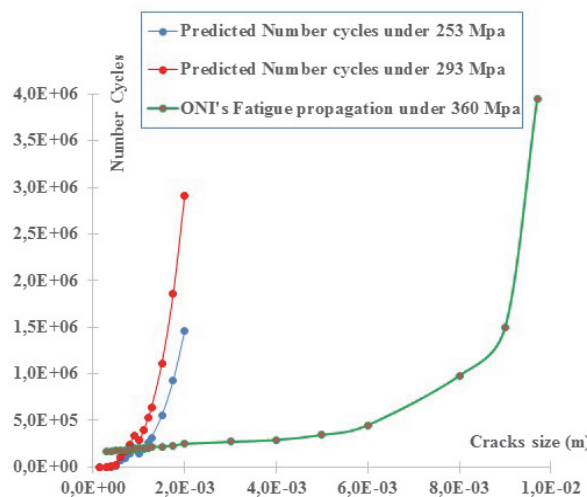However, we compute the number cycles N_f (Eq. 15) in Mathematica. The results are presented in (Fig. 4)

Figure 4: Number cycles for small crack and Oni's long crack for 30NCD16 steel

Fatigue propagation notes of ONI [12, 14] give 0.25×10^6 Cycles for crack length 2 mm.

Our prediction for the same crack size when it can be blocked by a microstructural barrier (grain boundary, for example) gives $N_f = 2.91 \times 10^6$ Cycles.

This is of paramount importance for components, such as gas turbine engine and blades, where fatigue life is dominated by physically small crack growth can be long under critical stress σ*.

CONCLUSION

T he following results of the critical stress **σ*** and fatigue small crack effect are:

- An over-energy under dissymmetrical rotating bending is used to predict the fatigue critical stress below the endurance limit.
- We show that these critical stress and small crack are governed in good agreement with Kitagawa diagram trend.
- The physically small crack, usually nucleate on planes of shear stress, can significantly reduce the fatigue life of the engineering structures.

Nevertheless the capabilities of this method are very promising. Further investigations will aim to validate these results by experimental processes and microscopic observations.

REFERENCES

[1] Palin-Luc, T., Lasserre S., Berard, J.Y., Experimental investigation on the significance of the conventional endurance limit of a spheroidal graphite cast iron, Fat. & Fracture of Eng. Mat. & Str, 21 (1988) 191-200.

[2] Banvillet, A., Palin-Luc, T., Lasserre, S., A volumetric energy based high cycle multiaxial fatigue criterion. Int. J. Fatigue, 25 (2003) 755-769.

[3] Froustey, C., Lasserre, S., Multiaxial fatigue endurance of 30NCD16 steel. Int. J. Fatigue, 113 (1989) 169-175.

[4] Manning, S.D., Yang, J.N., Advanced Durability Analysis, Volume I Analytical Methods. AFWAL-TR-86-3017, Air Force Wright Aeronautical Laboratories (1987).

[5] Stephens R.I., Fatemi, A., Stephens, R.R., Fuchs H.O., Metal Fatigue In Engineering, 2d edition, Wiley Inter-science Publication, (2001).

[6] Kitagawa, H., Takahashi, S., Applicability of Fracture Mechanics to Very Small Cracks or the Cracks in the Early Stage. Proceeding of the second Int. Conf. on Mechanical behavior of Materials, American Society for Metals, Metal Park, OH, (1976) 627-702.

[7] Bazant, Z.P., Scaling of quasi brittle fracture: asymptotic analysis. Int. J. Fracture, 83 (1997) 19-40.

[8] Tanaka, K., Nakai, Y., Yamashita, Y., Fatigue Growth Threshold of Small Cracks, Int. J. Fracture, 17 (1981) 519-533.

[9] Livieri, P., Tovo, R., Fatigue Limit Evaluation of Notches, Small and Defects: An Engineering Approach. Fatigue & Fracture of Engineering Materials & Structures, 27 (2004) 1037-1049.

[10] Standard Test Method for Measurement of Fatigue Crack Growth Rates, ASTM E647, 03.01, ASTM, West Conshohocken, PA, (2000) 591

[11] Hénaff, G., Petit J., Bouchet, B., Environmental influence on the near-threshold fatigue crack propagation behaviour of a high-strenth steel. Int. J. Fatigue, 14 (1992) 211-218.

[12] Oni, O., Bathias, C., A comparison of near-threshold fatigue crack propagation in two high strength steels, Fatigue & Fracture of Engineering Materials & Structures, 13 (1990) 585–596.

[13] Dubar, L., Froustey, C., Multiaxial fatigue of 30NCD16 Steel, Passage of the endurance to the limited endurance and taking into account of the geometrical accidents. PhD thesis, ENSAM Bordeaux, France (1992).

[14] Oni, O., Bathias, C., Contribution à l'étude des fissures courtes se propageant en fatigue dans les Aciers. PhD U.T.C Compiègne France, (1986).

NOMENCLATURE

$\sigma_{m,Te}$; σ_{Te}	Tensile mean stress and dynamic amplitude;
$\sigma_{Eq,Te}^2 = \sigma_{m,Te}^2 + \sigma_{Te}^2$	Equivalent stress under tensile loading;
W_{Te} ; ω_{Te}	Energy density and over-energy on the area S* under tensile loading
$\sigma_{m,Rb}$; σ_{Rb}	Rotating bending mean stress and dynamic amplitude;
$\sigma_{Eq,Rb}^2 = \sigma_{m,Rb}^2 + \sigma_{Rb}^2$	Equivalent stress under rotating bending;

W_{Rb} ; $\boldsymbol{\omega_{Rb}}$	Energy density and over-energy on the area S* under rotating bending
σ^*	Critical stress and their effect on physically small crack;
W^*	Energy supplied to the material at the critical stress;
$\sigma^{*2}_{Eq} = \sigma^2_{m,Te} + \sigma^{*2}$	Equivalent critical stress under axial loading;
$\sigma_{Te,-1}$; $\sigma_{Rb,-1}$	Endurance limit under fully alternate tensile and rotating bending
ω^D_{Uniax}	Over-energy value at the endurance limit;
$\omega_{Rb,d}$	Over-energy on the area S* under dissymmetrical rotating bending